Heterogeneous & Homogeneous & Bio- & Nano-

CHEMCATCHEM

CATALYSIS

Accepted Article

Title: Sulfonated hyper-cross-linked porous polyacetylene networks as versatile heterogeneous acid catalysts

Authors: Lada Sekerová, Pavlína Březinová, Thuy Tran Do, Eliška Vyskočilová, Jiří Krupka, Libor Červený, Lucie Havelková, Bogdana Bashta, and Jan Sedláček

To be cited as: *ChemCatChem* 10.1002/cctc.201901815

Link to VoR: http://dx.doi.org/10.1002/cctc.201901815

A Journal of

ChemPubSoc Europe

WILEY-VCH

www.chemcatchem.org

WILEY-VCH

FULL PAPER

Sulfonated hyper-cross-linked porous polyacetylene networks as versatile heterogeneous acid catalysts

Lada Sekerová[a]*, Pavlína Březinová[a], Thuy Tran Do[a], Eliška Vyskočilová[a]*, Jiří Krupka[a], Libor Červený[a], Lucie Havelková[b], Bogdana Bashta[b], Jan Sedláček[b]

Abstract: Two highly sulfonated micro/mesoporous polymers, P(1,3-DEB)-SO_3H and P(1,4-DEB)-SO_3H, with permanent porosity, the specific surface area about 550 $m^2 \cdot g^{-1}$ and the content of SO_3H groups of 2.7 $mmol \cdot g^{-1}$ were prepared as new acid Porous Polymer Catalysts, PPCs. The PPCs were achieved by easy sulfonation of parent hyper-cross-linked micro/mesoporous polyacetylene-type networks resulting from a chain-growth homopolymerization of 1,3- and 1,4-diethynylbenzenes. New PPCs are reported as highly active and reusable heterogeneous catalysts of esterification of fatty acids with methanol and ethanol, Prins cyclization of aldehydes with isoprenol and intramolecular Prins cyclization of citronellal to isopulegol. The catalytic activity of the micro/mesoporous PPCs (TON values up to 522 $mol \cdot mol^{-1}$) was higher than that of commercial polymer-based heterogeneous catalyst Amberlyst 15 possessing gel texture without permanent pores and that of *p*-toluenesulfonic acid applied as a homogeneous catalyst.

Introduction

The development of heterogeneous catalysts with permanent and well-defined porosity is one of the main goals of research in the field of catalysis. The Porous Polymer Catalysts, PPCs, represent a new, interesting and promising subclass of such heterogeneous catalysts.[1–8] The PPCs are insoluble and non-swellable polymers containing permanent pores in the size range of micropores and in some cases also mesopores and the catalytically active centres as the part of the micro/mesoporous surface. In terms of polymer architecture, the PPCs are highly aromatic polymer networks the permanent porosity of which results from the rigidity of the network segments and extensive cross-linking. Due to the permanent porosity, the PPCs are fundamentally different from conventional polymer supported catalysts based on solvent-swellable polymers.[9–12]

[a] MSc. L. Sekerová; MSc. P. Březinová, T.T Do, Prof. E. Vyskočilová; Prof. J. Krupka; Prof. L. Červený
Department of Organic Technology
University of Chemistry and Technology Prague
technicka 5, Prague 6, 166 28, Czech Republic
E-mail: lada.sekerova@vscht.cz; Eliska.vyskocilova@vscht.cz
[b] MSc. L. Havelková; Dr. Bogdana Bashta; Prof. J. Sedláček
Department of Physical and Macromolecular Chemistry, Faculty of Science
Charles University in Prague
Hlavova 2030, Prague, 128 43, Czech Republic

Supporting information for this article is given via a link at the end of the document.

The preparation of PPCs utilizes organic and polymer synthesis techniques, which makes possible to prepare PPCs with a wide spectrum of covalent structures distinguishing thus PPCs from compositionally less variable heterogeneous catalysts based on inorganic porous materials.[13–15]

The diversity of synthetic paths for the preparation of PPCs has been well documented in publications dealing with the preparation of organometallic PPCs containing covalently bonded well-defined and catalytically active organometallic complexes. For example, Ru and Ir complexes with ethynylated 2,2´-bipyridine ligands were directly copolycyclotrimerized with tetrakis(4-ethynylphenyl)methane into organometallic PPCs of the Brunauer-Emmett-Teller surface area, S_{BET} up 1500 $m^2 \cdot g^{-1}$, which were active for aza-Henry reactions and oxyamination of aldehydes.[16] The PPCs with bipyridine-containing organometallic segments were also obtained by direct step-growth condensation polymerization of metallated 2,2´-bipyridine-5,5´-dicarbaldehyde with melamine cross-linker (S_{BET} up 450 $m^2 \cdot g^{-1}$).[17] Xie et al. reported preparation of organometallic PPCs (S_{BET} = 965 $m^2 \cdot g^{-1}$) from 1,3,5-triethynylbenzene and dibrominated pro-ligand of Salen-type [Salen = *N*,*N*´-bis(salicylidene)ethylenediamine] through the direct step-growth polymerization performed by means of Sonogashira coupling and followed by metallation of the parent networks with Co^{2+} ions.[18] The same synthetic approaches were used for the preparation of metal-free organocatalysts of PPC-type. The direct copolycyclotrimerization was used for preparing PPCs (S_{BET} up to 731 $m^2 \cdot g^{-1}$) with *N*-heterocyclic carbenes serving as catalytically active centres of reductive *N*-formylation of amines with CO_2.[19] The poly(aryleneethynylene)-type PPCs functionalized with Tröger's base (S_{BET} = 750 $m^2 \cdot g^{-1}$) were prepared from 1,3,5-triethynylbenzene and diiodinated Tröger's base monomers through direct step-growth polymerization performed by means of Sonogashira coupling.[20] The direct copolymerization through Suzuki–Miyura coupling and tetrakis(4-bromophenyl)ethane, 2,7-dibromo-9-fluorenone, and 1,4-benzene diboronic acid comonomers were used to prepare donor-acceptor PPCs highly efficient towards hydrogen evolution.[21] In the case of the above-mentioned PPCs prepared by direct polymerizations, the organometallic or heteroatomic segments of the PPCs served not only as catalytically active centres, but simultaneously participated (as the rigid network struts) in the formation of the porous texture of the PPCs. This positively influenced the specific surface area of PPCs.

Nevertheless, the PPCs with catalytically active centres in the pendant groups were also prepared by direct polymerization, however, their specific surfaces were lower. For example, the copolymerization of tetrakis(4-ethynylphenyl)methane and 1,3-dibromobenzene substituted in position 5 by a pyrrolidine derivative performed through Sonogashira coupling provided PPC of S_{BET} = 228 $m^2 \cdot g^{-1}$, which was active in the asymmetric Michael addition.[22]

The second method for the preparation of PPCs is a two-step synthesis in which a porous polymer network is first synthesized and functionalized in the second step by catalytically active groups. The postpolymerization modification must be properly optimized so that the polymer network, after modification, retains a satisfactory porous texture, in particular, a sufficient specific surface area. Wang et al. described the synthesis of microporous poly(aryleneethynylene) networks (S_{BET} from 110 to 529 $m^2 \cdot g^{-1}$) subsequently modified into PPCs by radical thiol-yne reaction with aminothiols accompanied by a negligible change in S_{BET}.[23] Recently, we reported the synthesis of micro/mesoporous polyacetylene network decorated with aldehyde groups by means of chain-growth polymerization of 3,5-diethynylbenzaldehyde (S_{BET} = 916 $m^2 \cdot g^{-1}$). The parent network was transformed by condensation reaction with ethylenediamine into NH_2 groups bearing PPC organocatalyst (S_{BET} = 649 $m^2 \cdot g^{-1}$) active in aldol condensation.[24] Several articles described the preparation of acid PPCs by means of sulfonation of aromatic segments of parent porous networks. The step-growth knitting polymerization of various arenes (carbazole,[25] phenol, bisphenol A and 2-naphthol[26,27] and truxene[28]) was used to prepare parent microporous networks, which were subsequently sulfonated by chlorosulfonic acid to PPCs decorated with SO_3H groups in the amount of from 0.85 to 3.7 $mmol \cdot g^{-1}$. The S_{BET} values of sulfonated PPCs (from 180 to 719 $m^2 \cdot g^{-1}$) were 50 to 60 % lower than those of the parent networks. The PPCs were active in esterification or acylation reactions. The SO_3H groups-containing PPC [S_{BET} = 406 $m^2 \cdot g^{-1}$, 2.3 $mmol(SO_3H) \cdot g^{-1}$] was also prepared by sulfonation of the microporous network (S_{BET} = 903 $m^2 \cdot g^{-1}$) prepared by radical chain-growth copolymerization of divinylbenzene and triallylamine.[29] Du et al. studied the influence of pore size distribution of SO_3H-containing PPCs on their activity in the fructose conversion to 5-hydroxymethylfurfural.[30] The authors revealed the PPCs with a hierarchical texture containing both micro- and mesopores to be more efficient than PPCs containing only micropores. Most probably the mesopores of PPCs facilitated the accessibility of catalytic centres for the substrate molecules. To introduce mesopores into the networks, Du. et al. applied an aerogel template approach.[31]

Recently we reported the chain-growth polymerization of diethynylarenes as a powerful tool for template-free preparation of texturally hierarchized micro/mesoporous hyper-cross-linked networks.[8,32,33] In this article we report (i) the networks of this type prepared from commercially available 1,3-diethynylbenzene (1,3-DEB) and 1,4-diethynylbenzene (1,4-DEB) monomers, (ii) the smooth postpolymerization sulfonation of parent networks into acid PPCs proceeding under preservation of micro/mesoporous texture and (iii) the catalytic activity of sulfonated PPCs in esterification of fatty acids and Prins cyclization reactions.

Results and Discussion

Preparation and characterization of sulfonated PPCs

Two phenylene-rich hyper-cross-linked microporous polymer networks, poly(1,4-diethynylbenzene), P(1,4-DEB) and poly(1,3-diethynylbenzene), P(1,3-DEB) were prepared as parent materials for the modification by sulfonation (Scheme 1). The networks were synthesized by the chain-growth homopolymerizations of respective monomers, 1,4-DEB and 1,3-DEB as described previously.[32,34] Prepared P(1,4-DEB) and P(1,3-DEB) consisted of the polyene (polyacetylene) chains hyper-cross-linked by either 1,4-phenylene or 1,3-phenylene links, as shown in Scheme 1.

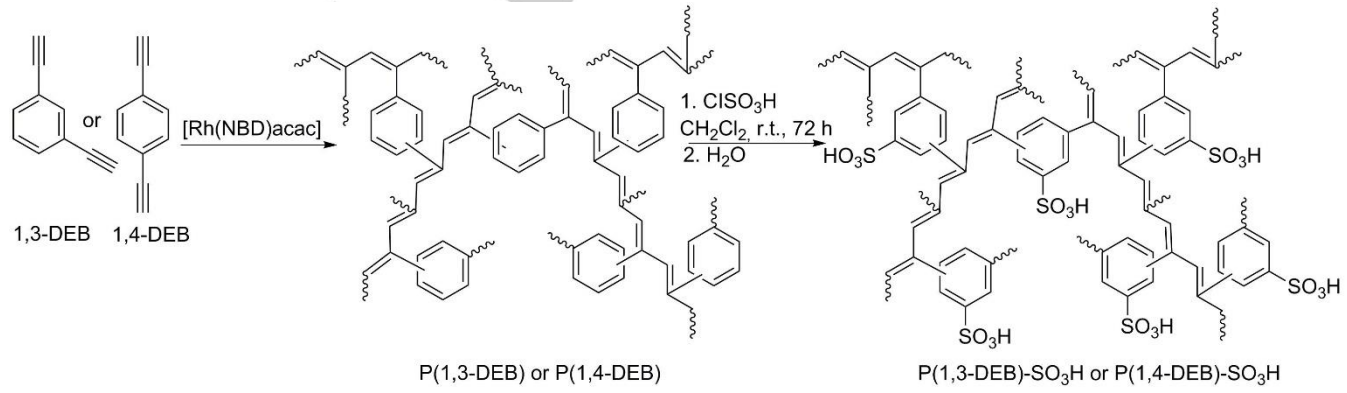

Scheme 1. Synthesis of parent networks P(1,4-DEB) and P(1,3-DEB) and their sulfonation into P(1,4-DEB)-SO_3H and P(1,3-DEB)-SO_3H

The parent P(1,4-DEB) and P(1,3-DEB) were sulfonated by using chlorosufuric acid in DCM (see Experimental part) under conditions applied by Bhaumik et al. for the sulfonation of the microporous networks containing carbazole and benzene building blocks.[25] The sulfonated networks were labelled as P(1,4-DEB)-SO_3H and P(1,3-DEB)-SO_3H. Table 1 shows the amount of SO_3H groups introduced into P(1,4-DEB)-SO_3H and P(1,3-DEB)-SO_3H as a function of the amount of chlorosulfuric acid supplied for the sulfonation of P(1,4-DEB) and P(1,3-DEB). It is obvious that even less than half (150 mmol·$g^{-1}_{network}$) of chlorosulfonic acid applied by Bhaumik (375 mmol·$g^{-1}_{network}$) may be used for sulfonation of P(1,4-DEB) and P(1,3-DEB) to achieve the same concentration of SO_3H groups in the sulfonated PPCs (2.7 mmol·g^{-1}_{PPC}). The difference between the concentration of SO_3H groups in P(1,4-DEB)-SO_3H and P(1,3-DEB)-SO_3H was insignificant. The concentration of SO_3H groups of 2.7 mmol·g^{-1}_{PPC} achieved in both P(1,4-DEB)-SO_3H and P(1,3-DEB)-SO_3H means that 43 % of monomeric units in these PPCs were sulfonated. The smoothness of sulfonation was apparently supported by the presence of mesopores in P(1,4-DEB) and P(1,3-DEB) facilitating the transport of the sulfonating agent.

For detail characterization and catalytic testing, the samples P(1,4-DEB)-SO_3H No. 1 (Table 1) and P(1,3-DEB)-SO_3H No. 5 (Table 1) were chosen.

Table 1. The amount of SO_3H groups in sulfonated PPCs as a function of the amount of chlorosulfonic acid used for sulfonation of P(1,4-DEB) and P(1,3-DEB). Reaction time 3 days, room temperature

Network	No	Amount of $ClSO_3H$ used for sulfonation mmol·$g^{-1}_{network}$	Amount of SO_3H functional groups mmol·g^{-1}_{PPC}[a]
P(1,4-DEB)-SO_3H	1	375	2.7
	2	150	2.8
	3	75	2.2
	4	3	1.6
P(1,3-DEB)-SO_3H	5	375	2.7
	6	150	2.7
	7	75	2.4
	8	3	1.1

[a] based on the content of sulfur determined by elemental analysis

Figure 1 shows the FTIR spectra of the parent and sulfonated networks. Spectra of both P(1,4-DEB)-SO_3H and P(1,3-DEB)-SO_3H contained strong bands at about 1040 cm^{-1} and 1220 cm^{-1} corresponding to C-S and O=S=O stretching vibrations of SO_3H groups, respectively.[35] The broad bands covering the range of about 2800 - 3700 cm^{-1} in the spectra of P(1,4-DEB)-SO_3H and P(1,3-DEB)-SO_3H were due to OH groups from both non-hydrated and hydrated SO_3H substituents. The FTIR spectra of P(1,4-DEB)-SO_3H and P(1,3-DEB)-SO_3H exhibited the same bands as ring-sulfonated linear poly(diarylacetylene)s prepared through postpolymerization sulfonation by Sakaguchi et al.[36,37]

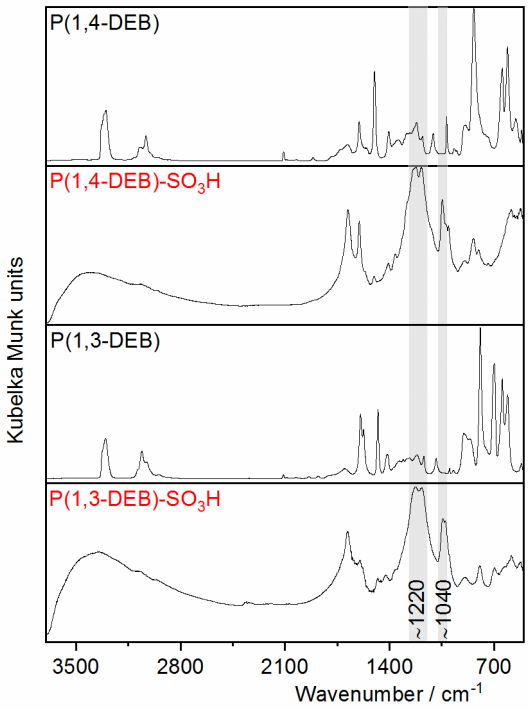

Figure 1. FTIR spectra of parent and sulfonated networks

The nitrogen adsorption/desorption isotherms (77 K) shown in Figure 2 confirmed the porous texture of P(1,4-DEB) and P(1,3-DEB) and indicated that P(1,4-DEB) and P(1,3-DEB) contained both micropores and mesopores. The presence of micropores was evident from the steep increase in the adsorbed amount in the initial adsorption stage. The presence of mesopores was indicated both by the increase of adsorbed amount at p/p_0 > 0.8 and the hystereses of adsorption-desorption isotherms. The specific surface area, S_{BET}, of P(1,4-DEB) and P(1,3-DEB) was about 1200 $m^2 \cdot g^{-1}$, the values of micropore volume, V_{mi} and total pore volume, V_{tot} are in Table 2.

The nitrogen adsorption/desorption isotherms on P(1,4-DEB)-SO_3H and P(1,3-DEB)-SO_3H showed that both networks retained permanent porosity even after extensive sulfonation (Figure 2). However, the S_{BET} values of the sulfonated networks (~ 550 $m^2 \cdot g^{-1}$) were about 50 % lower than the S_{BET} values of the parent P(1,4-DEB) and P(1,3-DEB). The values of V_{mi} and V_{tot} decreased to a similar extent due to the sulfonation (Table 2). Nevertheless, the shapes of the nitrogen adsorption/desorption isotherms of the parent and sulfonated networks were very similar (Figure 2) and the V_{mi}/V_{tot} ratios of the parent and sulfonated networks were virtually identical (Table 2). Thus, the total pore volume of the sulfonated networks was similarly contributed by mesopores as in the case of their parent counterparts. Figure S1 (in Supplementary material) shows the comparison of

micropore size distribution of parent and sulfonated networks. The sulfonation resulted in a slight shift of the maxima of distributions towards higher micropore diameters most likely due to the partial disappearance of the smallest micropores caused by their occupation with SO_3H groups.

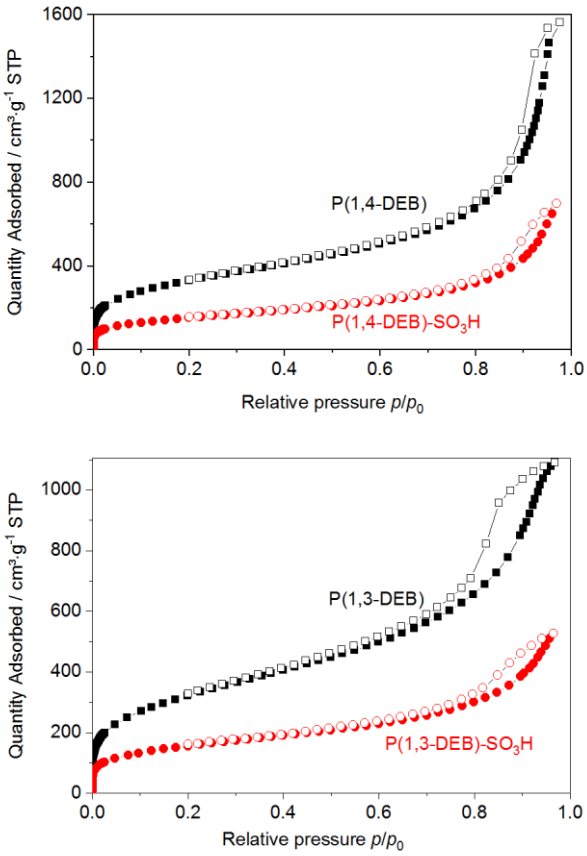

Figure 2. N_2 adsorption (full points) and desorption (empty points) isotherms (77 K) on parent and sulfonated networks.

Table 2. Specific surface area, S_{BET}, micropore volume V_{mi} and total pore volume V_{tot} of parent and sulfonated networks

Network	S_{BET} $m^2 \cdot g^{-1}$	V_{mi} $cm^3 \cdot g^{-1}$	V_{tot} $cm^3 \cdot g^{-1}$	V_{mi}/V_{tot}
P(1,4-DEB)	1204	0.43	2.43	0.18
P(1,4-DEB)-SO_3H	552	0.21	1.09	0.19
P(1,3-DEB)	1181	0.42	1.69	0.25
P(1,3-DEB)-SO_3H	564	0.21	0.82	0.26

The sulfonation did not modify the morphology of the networks at least not to the extent, which could be detected by Scanning Electron Microscopy, SEM: Figure 3 shows the SEM images of parent and sulfonated networks, which all consisted of aggregated particles with diameter from 20 to 50 nm.

Figure S2 (in Supplementary material) shows the Thermogravimetric Analysis (TGA) thermograms of parent and sulfonated networks. Evidently, the sulfonated networks were thermally less stable (weight loss of about 40 % at 500 °C, Figure 4, A and B) than the parent ones (weight loss up to 10 % at 500 °C). The TGA coupled with mass spectrometry revealed that water and sulfur dioxide were the dominant gaseous compounds evolved in the course of P(1,4-DEB)-SO_3H and P(1,3-DEB)-SO_3H heating (see Figure 4).

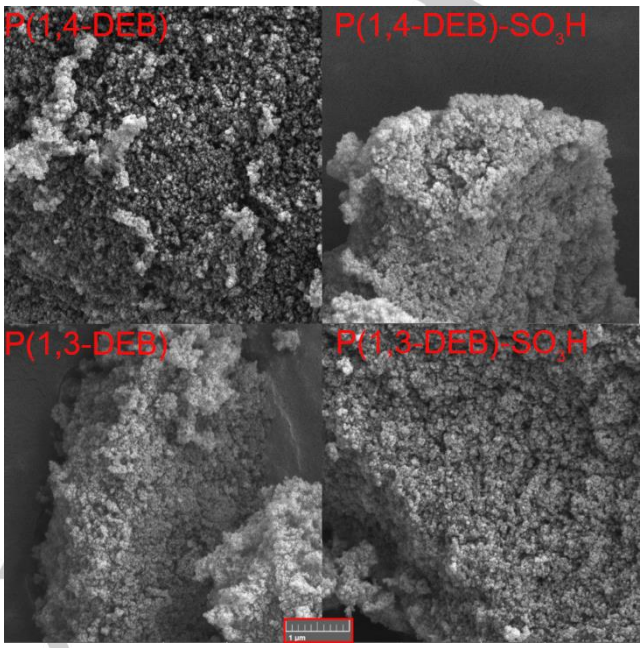

Figure 3. SEM images of parent and sulfonated networks

The water was released in the temperature range from 100 to 300 °C in two steps manifested by two maxima on the respective curves in Figure 4.[27] At the lower temperature (about 100 °C), desorption of the water trapped by the physisorption proceeded. At higher temperature, most probably the water molecules, which hydrated the SO_3H groups were released. The observed release of the water confirmed the expected hygroscopicity of P(1,4-DEB)-SO_3H and P(1,3-DEB)-SO_3H originating from the high content of SO_3H groups in these materials. The release of SO_2 from P(1,4-DEB)-SO_3H and P(1,3-DEB)-SO_3H proceeded in a temperature range of 150 °C to 450 °C (see Figure 4). The SO_2 release indicated the decomposition of P(1,4-DEB)-SO_3H and P(1,3-DEB)-SO_3H, limiting their use to temperatures ≤ 150 °C.

The temperature programmed desorption (TPD) of pyridine was used to determine the surface acidity of P(1,4-DEB)-SO_3H and P(1,3-DEB)-SO_3H. Considering the results of TGA measurements, P(1,4-DEB)-SO_3H and P(1,3-DEB)-SO_3H were thermally pre-treated at 160 °C (for 1 h). The saturation by pyridine was performed at the temperature of 150 °C.[38] The pyridine desorption provided the following concentrations of the acid centres: 1.30 $mmol \cdot g^{-1}$ for P(1,4 DEB)-SO_3H and 1.23 $mmol \cdot g^{-1}$ for P(1,3-DEB)-SO_3H. As can be seen, the acid centre concentrations were virtually identical for both sulfonated networks. A comparison of the concentration of the acid centres determined by the TPD method and the concentration of SO_3H groups in P(1,4-DEB)-SO_3H and P(1,3-DEB)-SO_3H (2.7 $mmol \cdot g^{-1}$ by elemental analysis, see Table 2) showed that about 45% of the SO_3H groups of the sulfonated networks were accessible

for pyridine molecules. It should, however, be noted that P(1,4 DEB)-SO_3H and P(1,3-DEB)-SO_3H exhibited a higher concentration of acid centres than classical heterogeneous catalysts of the zeolite-type.[38–40] Due to the reduced thermal stability of P(1,4-DEB)-SO_3H and P(1,3-DEB)-SO_3H the desorption of pyridine (proceeding at temperature > 150 °C) was accompanied by the decomposition of the sulfonated networks (*vide supra*). In view of this, it was not possible to determine the strength of the acid centres of P(1,4-DEB)-SO_3H and P(1,3-DEB)-SO_3H.

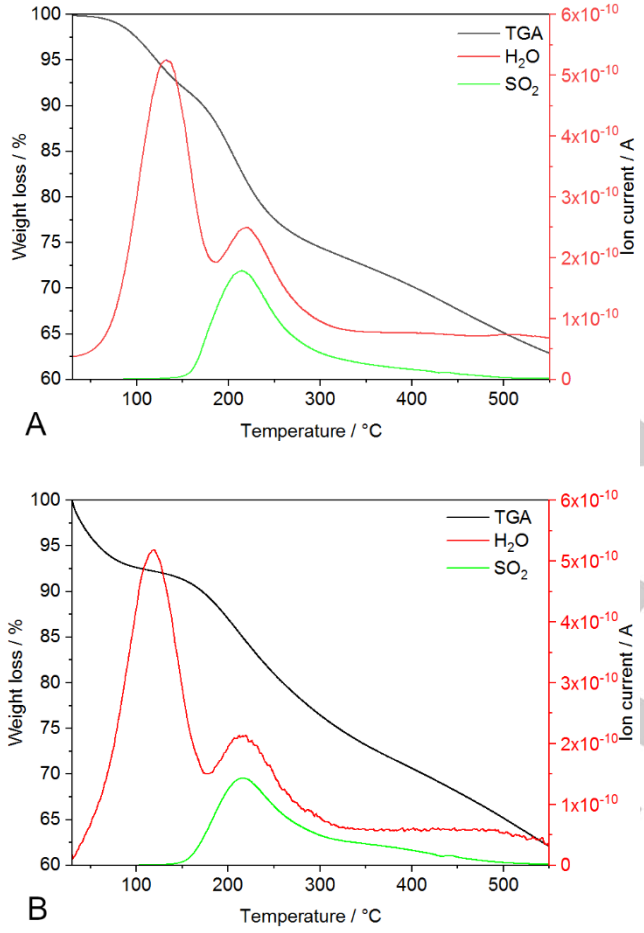

Figure 4. Temperature profiles of H_2O and SO_2 releasing from P(1,4-DEB)-SO_3H (A) and P(1,3-DEB)-SO_3H (B) in the course of their heating. The temperature profiles were determined by TGA coupled with mass spectrometry.

Catalytic activity

The prepared sulfonated networks [P(1,4-DEB)-SO_3H and P(1,3-DEB)-SO_3H] were tested as PPC-type heterogeneous catalysts in three types of typically acid catalysed reactions: esterification of higher fatty acids by low-chain alcohols, Prins cyclization of various aldehydes with isoprenol and cyclization of citronellal. The catalytic activity of P(1,4-DEB)-SO_3H and P(1,3-DEB)-SO_3H was compared with that of Amberlyst 15 [sulfonated poly(styrene-*co*-divinylbenzene), exchange capacity > 1.7 meq·ml^{-1}];[41] and *p*-toluenesulfonic acid (*p*-TSA) applied as homogeneous catalyst (pK_a = -5.4 (measured in H_2O; [42]).

Esterification of higher fatty acid by low-chain alcohols (Scheme 2) can be used for the production of biofuels (e.g. methyl esters of colza oil). The homogeneous catalysts such as sulfuric or *p*-toluenesulfonic acids, which are known to be corrosive and environmentally unfriendly, are commonly used to catalyse this reaction. The use of heterogeneous catalysts can be beneficial owing to the easy separation of the catalyst from the reaction mixture as well as the possible reuse of the catalyst. Due to this fact large variety of heterogeneous catalysts was studied in esterification od various carboxylic acids with various alcohols including recently published [e.g.43,44] sulfonated copolymers of styrene and divinylbenzene.

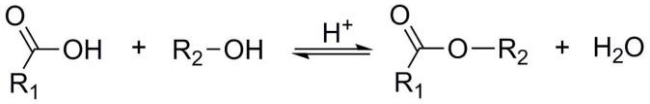

Scheme 2. Reaction scheme of esterification

The results we achieved in the study of esterification reactions are summarized in (Fig 5 and 6, Table 3). Respective esters (methyl-, ethyl- or isopropyl-) of the higher fatty acids (lauric, myristic, oleic, palmitic or stearic) were the only products detected in the reaction mixtures.

The esterification of lauric acid by methanol was used as the model reaction. The results showed that both P(1,4-DEB)-SO_3H and P(1,3-DEB)-SO_3H were more active in this reaction than the commercial heterogeneous catalyst Amberlyst 15 applied at the same weight concentration (see the conversion curves in Figure 5, A). It was despite the fact that the concentration of acid centres was higher in Amberlyst 15 (2.4 mmol·g^{-1}) than in P(1,4-DEB)-SO_3H and P(1,3-DEB)-SO_3H (~1.3 mmol·g^{-1}). We believe that the permanent micro/mesoporous texture of PPC-type P(1,4-DEB)-SO_3H and P(1,3-DEB)-SO_3H allowed the reactants to access the catalytic centres more efficiently than they did with the swollen Amberlyst 15 possessing an unstable gel texture without permanent pores. P(1,4 DEB)-SO_3H and P(1,3-DEB)-SO_3H showed very similar catalytic activity in the esterification of lauric acid by methanol (see Figure 5, A). This is consistent with the fact that both newly prepared PPCs exhibited (i) a practically equal concentration of acid centres and (ii) very similar porous texture parameters (Table 2). The esterification of lauric acid by methanol proceeded with the highest initial reaction rate if it was catalysed with *p*-TSA applied in the same weight concentration as the above discussed heterogeneous catalysts (see conversion curves in Figure 5, A). However, this mainly reflected the high concentration of acid centres in *p*-TSA (5.3 mmol·g^{-1}). When comparing the Turn Over Number (TON) values (Table 3), it is apparent that *p*-TSA exhibited lower catalytic activity in

the studied esterification (TON = 86 mol·mol^{-1}) than P(1,4-DEB)-SO_3H and P(1,3-DEB)-SO_3H (TON ~ 400 mol·mol^{-1}). The higher activity of prepared sulfonated micro/mesoporous networks was not so surprising, because less acidic sulfonated mesoporous MCM-41 was previously described as a more active heterogeneous catalyst for esterification of fatty acids in comparison to homogeneously applied *p*-TSA.[45]

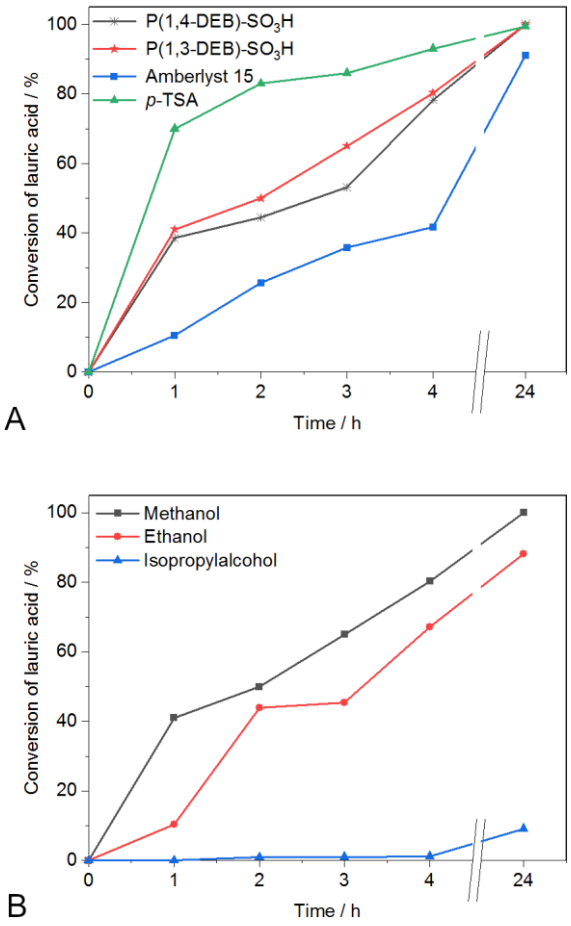

Figure 5. The time course of lauric acid conversion in the esterification of lauric acid by methanol using various catalysts; 100 mg of acid, 1 wt.% of catalyst, 3 ml of methanol, reflux (A) and esterification of lauric acid by various alcohols (methanol, ethanol, isopropyl alcohol) using P(1,3-DEB)-SO_3H as a catalyst; 100 mg of acid, 1 wt.% of catalyst, 3 ml of alcohol, reflux (B)

Various short-chain alcohols (methanol, ethanol, isopropyl alcohol) were used for esterification of lauric acid with P(1,3-DEB)-SO_3H catalyst (Figure 5, B). Both the achieved conversions at 1 h (Figure 5, B) and the TON values (Table 3) decreased in the order methanol > ethanol >> isopropyl alcohol, which was in good agreement with literary data for the esterifications catalysed with other catalysts.[46] Various higher fatty acids (C_{12} – C_{18}) were used as substrates for esterification by methanol catalysed with P(1,3-DEB)-SO_3H (see Figure 6 and Table 3). For all the acids tested, the total conversion was achieved within 24 hours. The reaction courses did not exhibit any systematic dependence on the chain length and nature (saturated/unsaturated) of the fatty acids. It should be noted that the total conversion of all mentioned fatty acids was achieved within 1 h if the concentration of P(1,3-DEB)-SO_3H catalyst of 10 wt.% was used.

Table 3. Turn over numbers of esterification of various higher fatty acids by low-chain alcohols using various catalysts; 0.5 mmol of acid, 1 wt.% of catalyst, 3 ml of alcohol, reflux

Catalyst	Acid	Alcohol	Conc.of acid centres mmol·g^{-1}	TON 24 h mol·mol^{-1}
p-TSA	Lauric	Methanol	5.81	86
Amberlyst 15			2.40	212
P(1,4-DEB)-SO_3H			1.30	393
P(1,3-DEB)-SO_3H			1.23	406
		Ethanol		358
		Isopropylalcohol		37
	Myristic	Methanol		390
	Palmitic			378
	Stearic			393
	Oleic			393

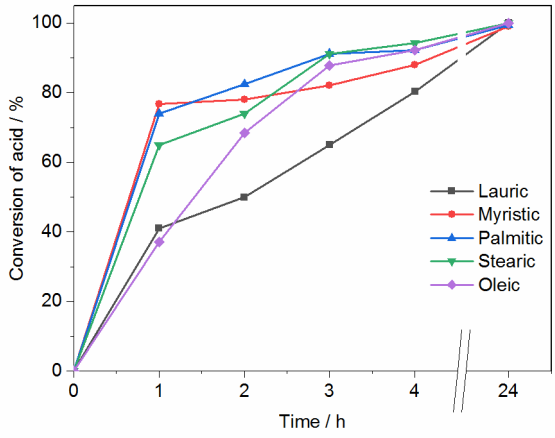

Figure 6. Time course of the conversion of acid in the esterification of various acids (lauric, myristic, palmitic, stearic, oleic) by methanol using P(1,3-DEB)-SO_3H as a catalyst; 0.5 mmol of acid, 1 wt.% of catalyst, 3 ml of methanol, reflux

Prins cyclization is an important reaction in the production of heterocyclic compounds (containing atoms of oxygen, sulfur or nitrogen in the ring), which are very often used as intermediates in syntheses of e.g. pharmaceuticals or fragrant compounds. Prins cyclization can be catalysed by both Lewis acids (e.g. methyltrioxorhenium or $FeCl_3$)[47,48] and Brønsted acids (e.g. *p*-toluenesufonic acid or heteropoly acids)[49,50] The Prins cyclization of benzaldehyde with isoprenol was chosen as a model reaction (Scheme 3 A) for the evaluation of catalytic activity of P(1,4-DEB)-SO_3H and P(1,3-DEB)-SO_3H PPCs (Table 4). Both newly prepared PPCs were significantly more active in this reaction

compared to commercial Amberlyst 15 and *p*-TSA catalysts (Table 4).

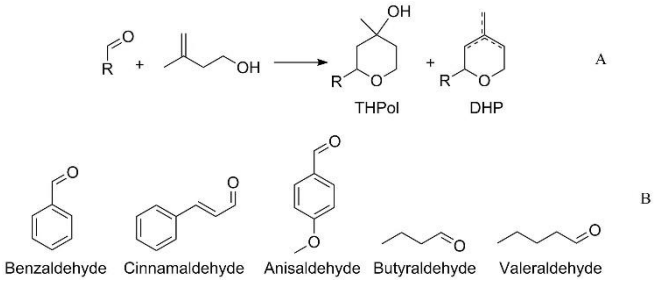

Scheme 3. Reaction scheme of Prins cyclization of aldehyde with isoprenol forming substituted tetrahydropyranol (THPol) or dihydropyranes (DHP) as main products (A) and structures of various aldehydes used as substrates for Prins cyclization with isoprenol (B)

The conversion of benzaldehyde of 80% was achieved within 30 min with P(1,4-DEB)-SO_3H or P(1,3-DEB)-SO_3H, while the time to achieve this conversion was significantly longer using both Amberlyst 15 (24 h) and *p*-TSA applied as homogeneous catalyst (4 h). The cyclization under study provided two expected products: substituted tetrahydropyranol (THPol) and substituted dihydropyranes (DHP) (see Scheme 3). The DHP/THPol mole ratios were 7.3 and 3.8 with Amberlyst 15 and *p*-TSA, respectively, whereas both P(1,4-DEB)-SO_3H and P(1,3-DEB)-SO_3H provided the DHP/THPol ratio of about 1.4 (data corresponding to the conversion of benzaldehyde of 80 % are reported). The preference of formation of DHP can be caused by the acidity of used catalysts,[51] which induced the dehydration reaction. The DHP isomers were preferred using all mentioned catalysts, the selectivity to DHP isomers was the highest using Amberlyst 15 (87%) followed by *p*-TSA (72%) compared to p(1,4-DEB)-SO_3H (53%) and p(1,3-DEB)-SO_3H (54%). These results are in agreement with the fact that DHP isomers are the thermodynamic products of the reaction and THPol the kinetic one.[49]

Table 4. Prins cyclization of benzaldehyde with isoprenol using various catalysts; 1.2 mmol of isoprenol, 1.2 mmol of benzaldehyde; 10 wt.% of catalyst, 3 ml of toluene, 70 °C

Catalyst	80% Conversion of benzaldehyde			TON at 24 h
	Time to achieve h	Product selectivity %		mol·mol^{-1}
		THPol	DHP	
P(1,4-DEB)-SO_3H	0.5	38	53	79
P(1,3-DEB)-SO_3H	0.5	37	54	87
Amberlyst 15	24	12	87	39
p-TSA	4	19	72	19

Various aldehydes (Figure 7) were used as the substrates for Prins cyclization with isoprenol (Figure 7, Table 5) with P(1,3-DEB)-SO_3H catalyst. The initial reaction rates were mostly higher when aliphatic aldehydes (butyraldehyde 21.6 mol·l^{-1}·min^{-1}·g$^{-1}_{cat}$, valeraldehyde 16.0 mol·l^{-1}·min^{-1}·g$^{-1}_{cat}$) were used as the substrates compared to the initial reaction rates achieved with benzene ring-containing aldehydes (cinnamaldehyde 5.9 mol·l^{-1}·min^{-1}·g$^{-1}_{cat}$, anisaldehyde 4.0 mol·l^{-1}·min^{-1}·g$^{-1}_{cat}$, benzaldehyde 16.3 mol·l^{-1}·min^{-1}·g$^{-1}_{cat}$). But the main reason why the total conversion of the latter mentioned aldehydes to the desired products was not achieved was the consumption of isoprenol for the formation of acetals with these aldehydes. This is in good agreement with our previous findings.[52] The almost total conversion of aliphatic aldehydes was achieved within 1 h while using anisaldehyde and cinnamaldehyde as the substrates only 80% conversion of these compounds was achieved after 4 h of the reaction. The selectivity to DHP isomers seemed to be independent on the aldehyde structure.

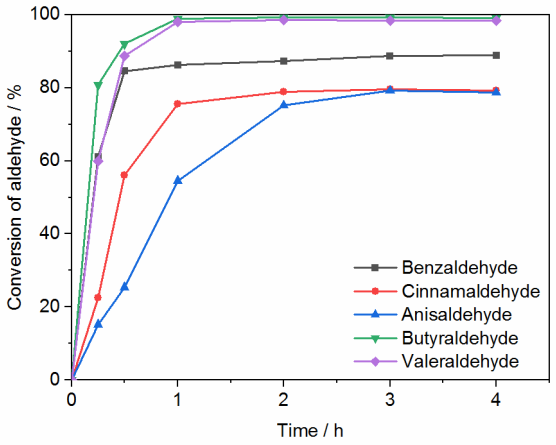

Figure 7. Time course of conversion of aldehyde in Prins cyclization of various aldehydes (benzaldehyde, cinnamaldehyde, anisaldehyde, butyraldehyde and valeraldehyde) with isoprenol using P(1,3-DEB)-SO_3H as a catalyst; 1.2 mmol of aldehyde and 1.2 mmol of isoprenol, 10 wt.% of P(1,3-DEB)-SO_3H, 3 ml toluene, 70 °C

Table 5. Selectivity to THPol and DHP isomers at 80% conversion of aldehyde using P(1,3-DEB)-SO_3H as a catalyst; 1.2 mmol of aldehyde and isoprenol, 10 wt.% of P(1,3-DEB)-SO_3H, 3 ml toluene, 70 °C

Aldehyde	Selectivity to products at 80% conversion of aldehyde %		TON 4 h mol·mol^{-1}
	THPol	DHP	
Benzaldehyde	37	54	84
Cinnamaldehyde	56	33	75
Anisaldehyde	49	42	74
Butyraldehyde	44	42	93
Valeraldehyde	46	45	93

The acid-catalysed intramolecular Prins cyclization of citronellal is an interesting reaction providing isopulegol as an important fragrant compound and intermediate for the synthesis of another fragrant compound, menthol (Scheme 4). Both Lewis acids (e.g. $ZnCl_2$ or ZrO_2) [53,54] and Brønsted acids (e.g. heteropolyacids)[55] can be used as the catalysts for this reaction.

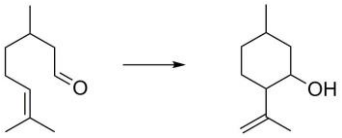

Scheme 4. Reaction scheme of cyclization of citronellal to isopulegol

Figure 8 and Table 6 show that P(1,4-DEB)-SO_3H and P(1,3-DEB)-SO_3H were highly active not only in esterification and Prins cyclization with isoprenol but also in the intramolecular cyclization of citronellal. Nearly quantitative conversion of citronellal and TON values over 500 mol·mol^{-1} were achieved with these catalysts after 4 h of the reaction, whereas the TON values resulting with Amberlyst 15 and *p*-TSA were only 131 and 52, respectively (Table 6). The selectivity to the desired product, isopulegol (determined at the citronellal conversion of 50 %) was about 90 % with the P(1,4-DEB)-SO_3H and P(1,3-DEB)-SO_3H catalysts. This was slightly lower than the selectivity to isopulegol achieved with *p*-TSA (100%). The decrease of selectivity to isopulegol was caused by the formation of the product of aldol condensation of two citronellal molecules.

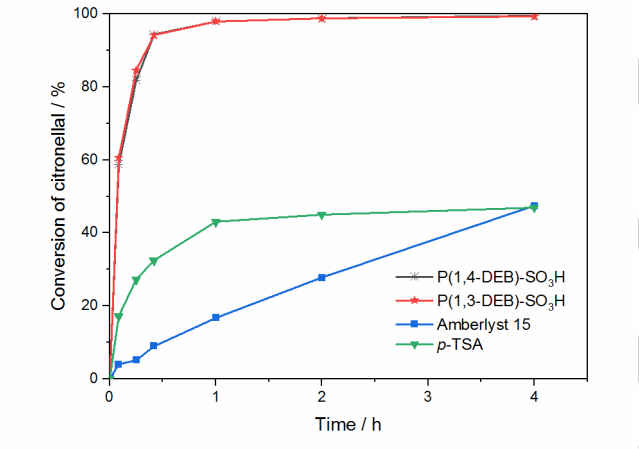

Figure 8 The time course of the conversion of citronellal through the cyclization catalysed with various catalysts; 200 mg citronellal, 1 wt.% of catalyst, 3 ml toluene, 40°C

Table 6. Selectivity to isopulegol at 50% conversion of citronellal

Catalyst	Selectivity to isopulegol %	TON 4 h mol·mol^{-1}
P(1,4-DEB)-SO_3H	91	508
P(1,3-DEB)-SO_3H	91	522
Amberlyst 15	88	131
p-TSA	100	52

As the general advantage of heterogeneous catalysts is that they can be easily separated from the reaction mixture and reused, the possibility of the multiple use of P(1,3-DEB)-SO_3H was tested in the cyclization of citronellal (Table 7). The catalyst was twice washed with 2 ml of toluene between each use. P(1,3-DEB)-SO_3H can be used in this model reaction three times without significant loss of activity. The small decrease (about 5%) in obtained yield of isopulegol at the third use may be caused by partial weight loss of the catalyst between the uses. The FTIR spectrum of P(1,3 DEB)-SO_3H catalyst which was used in the citronellal cyclization was identical to that of fresh P(1,3-DEB)-SO_3H (see Figure S3 in Supplementary material). This indicated that the covalent structure of P(1,3-DEB)-SO_3H remained unchanged after its catalytic application. However, a small decrease of –SO_3H functional groups content (from 2.6 mmol·g^{-1} to 2.0 mmol·g^{-1}) was observed after using the catalyst in the reaction, which can be induced by the presence of some reactants traces and is in consistence with the results obtained from N_2 adsorption/desorption measurement. The S_{BET} value of the used P(1,3-DEB)-SO_3H (262 m^{2}g^{-1}) was lower than the S_{BET} value of fresh P(1,3-DEB)-SO_3H (comparison of texture characteristics and N_2 adsorption/desorption isotherms of fresh and spent P(1,3-DEB)-SO_3H is available in Supplementary material, Table S1 and Figure S4). The decrease in S_{BET} most likely reflected the collapse or clogging of some of the pores by the reactants during catalytic application. Although some textural characteristics changed after the use of the catalyst in the reaction, it is important to note that P(1,3-DEB)-SO_3H can be repeatedly used in the studied reaction without significant loss of neither catalytic activity nor selectivity.

Table 7. Reuse of P(1,3-DEB)-SO_3H in intramolecular Prins cyclization of citronellal; 2 g of citronellal, 20 mg of P(1,3-DEB)-SO_3H, 30 ml of toluene, 40 °C, 25 min

Use	Yield of isopulegol %	Selectivity to isopulegol %
1.	81	88
2.	82	91
3.	76	94

Conclusions

The hyper-cross-linked micro/mesoporous polyacetylene-type networks with S_{BET} values about 1200 m^2·g^{-1} were prepared by chain-growth homopolymerization of commercially available 1,3-diethynylbenzene and 1,4-diethynylbenzene monomers. The permanent porosity of these networks allowed their easy sulfonation with chlorosulfonic acid into highly sulfonated acid PPCs with preserved micro/mesoporous texture (S_{BET} about 550 m^2·g^{-1}). The overall concentration of SO_3H groups in the sulfonated PPCs was 2.7 mmol·g^{-1}, the concentration of SO_3H groups accessible for pyridine probe molecules (thus for reactants) was about 1.3 mmol·g^{-1}. We have shown the newly prepared sulfonated PPCs to be highly active heterogeneous catalysts of esterification of fatty acids with methanol and ethanol (TON up to 400 mol·mol^{-1}), Prins cyclization of

10.1002/cctc.201901815

aldehydes with isoprenol (TON up to 90 mol·mol^{-1}) and intramolecular Prins cyclization of citronellal to isopulegol (TON up to 500 mol·mol^{-1}). Using the cyclization of citronellal the reusability of sulfonated PPCs was confirmed (used three times without significant loss of activity nor selectivity). The TON values achieved with sulfonated PPCs were higher than those resulting with commercial polymer-based heterogeneous catalyst Amberlyst 15 possessing gel texture without permanent pores. We believe, the high activity of the newly prepared sulfonated PPCs was apparently due to the high concentration of acid active centres and the combination of micropores and mesopores in these catalysts that facilitated the transport of the reactants to the active centres.

Experimental Section

Materials

All chemicals were used as obtained except for benzaldehyde (p.a., Penta, CZ) and dichloromethane (for HPLC, Sigma-Aldrich, CZ), which were distilled prior to the use. Citronellal (98 %) and cinnamaldehyde (98 %) were kindly provided by Aroma a.s. (CZ). 1,3-Diethynylbenzene (1,3-DEB) (>96 %), 1,4-diethynylbenzene (1,4-DEB) (>98 %) and (acetylacetonato)(norbornadiene)rhodium(I) ([Rh(nbd)acac]) were purchased from TCI Chemicals (CZ); butyraldehyde (>98 %) from Fluka (CZ); ethanol (96 %), isopropyl alcohol (p.a.), methanol (p.a.), oleic acid (86 %), palmitic acid (p.a.) and toluene (p.a.) from Penta (CZ); Amberlyst 15 (wet), chlorosulfonic acid (99 %), isoprenol (97 %), lauric acid (p.a.), myristic acid (>98 %) and stearic acid (95 %) from Sigma-Aldrich (CZ); valeraldehyde (97 %) from Acros Organics (CZ) and *p*-toluenesulfonic acid (*p*-TSA; monohydrate, p.a.) from Lachema (CZ). Anisaldehyde (98 %) was taken from UCT sources and demineralized water was produced by reverse osmosis at UCT Prague (<1 $\mu S \cdot mL^{-1}$).

Preparation of P(1,4-DEB)-SO_3H and P(1,3-DEB)-SO_3H

Hyper-cross-linked microporous polymer networks, poly(1,4-diethynylbenzene), P(1,4-DEB) and poly(1,3-diethynylbenzene), P(1,3-DEB) were prepared according to ref.[34]. The homopolymerizations of 1,4-DEB and 1,3-DEB monomers (initial concentration 0.6 $mol \cdot dm^{-3}$) were performed in dichloromethane at 75 °C [Rh(nbd)acac] complex (concentration 18 $mol \cdot dm^{-3}$) was used as a polymerization catalyst. The polymerizations gave quantitative yields of P(1,4-DEB) and P(1,3-DEB).

The sulfonation of P(1,4-DEB) and P(1,3-DEB) with chlorosulfonic acid was carried out through a modified method based on the procedure described in ref.[25]. The method was optimized with the aim to minimize the amount of chlorosulfonic acid submitted for sulfonation. A parent polymer network, P(1,4-DEB) or P(1,3-DEB), (200 mg) was dispersed in anhydrous DCM (50 ml or less) and kept under stirring (600 rpm) at 0 °C for 30 min. Then chlorosulfonic acid (5 mL or less) was added dropwise. The dispersion was continuously stirred for 3 days at room temperature. The obtained black powder [P(1,4-DEB)-SO_3H or P(1,3-DEB)-SO_3H] was filtered and repeatedly washed with 150 ml of demineralized water until the neutral filtrate was obtained. After that, the powder was transferred into the round bottom flask equipped with Dimroth condenser, demineralized water (150 ml) was added and kept under stirring at reflux for 1 h. This procedure was repeated two times. Finally, the product was dried under reduced pressure (100 Pa) at 80 °C.

Catalytic test

P(1,4-DEB)-SO_3H and P(1,3-DEB)-SO_3H were tested as acid heterogeneous catalysts in three model typically acid catalysed reactions: Prins cyclization of benzaldehyde with isoprenol, intramolecular Prins cyclization of citronellal and esterification of higher fatty acids by short-chain alcohols. The catalytic properties of P(1,4-DEB)-SO_3H and P(1,3-DEB)-SO_3H were compared with commercial SO_3H groups containing Amberlyst 15 wet and with *p*-toluenesulfonic acid.

All reactions were performed in glass flask (25 ml) equipped with Liebig condenser and placed at the magnetic stirrer (Ares, Velp Scientifica; 600 rpm) with a heating block (Heidolph; 5 place monoblock) and temperature regulator (VTF EVO, Velp Scientifica).

Esterification of higher fatty acids (lauric, myristic, oleic, palmitic, stearic) by short-chain alcohols (methanol, ethanol, isopropyl alcohol): appropriate amount of catalyst (1 wt.%, 1 mg), 3 ml of alcohol and 100 mg of acid were placed into the flask. All reactions were performed at the reflux of used alcohol.

Prins cyclization: appropriate amount of the catalyst (10 wt.%; 10 mg) was placed into the flask, isoprenol (100 mg, 1.2 mmol), aldehyde (benzaldehyde, butyraldehyde, valeraldehyde, anisaldehyde or cinnamaldehyde; 1.2 mmol), and toluene (3 ml) were added. The reactions were performed at 70 °C.

Cyclization of citronellal: appropriate amount of catalyst (1 wt.%, 2 mg) was placed to the flask and 3 ml of toluene and citronellal (200 mg) were added. The reaction temperature was 40 °C.

Techniques

Fourier transform IR spectra (FTIR) were measured on a Nicolet Magna IR 760 using the diffuse reflection mode. Samples were diluted by KBr before the measurement.

Thermogravimetric analysis (TGA) was performed on the Setsys Evolution apparatus (Setaram) under nitrogen atmosphere using heating rate 10 $°C \cdot min^{-1}$ in the temperature range 30 and 550 °C. Thermogravimetric analysis coupled with a mass spectrometer (TGA-MS) was performed on TG-DTA Setsys Evolution (Setaram, France) connected with quadrupole spectrometer OmniStarTM (Pffeifer Vacuum, Germany) under nitrogen atmosphere using heating rate 10 $°C \cdot min^{-1}$ in the temperature range 30 and 550 °C.

The nitrogen adsorption/desorption isotherms on the polymers were measured at 77 K using a Triflex V4.02 apparatus (Micromeritics). The Brunauer-Emmett-Teller specific surface area, S_{BET}, total pore volume, V_{tot} and micropore volume V_{mi} are reported. The V_{mi} values were determined on the base of N_2 amount trapped at $p/p_0 = 0.1$. Prior to the sorption measurements, all samples were degassed on a Micromeritics SmartVacPrep instrument as follows: starting from the

room temperature the sample was degassed at 353 K (heating ramp of 0.5 °C·min^{-1}). After 1 h delay at 353 K, the temperature was further increased up to 383 K with the same heating ramp and the sample was degassed for 5 h. After that tube with the sample was filled with N_2 and cooled down to room temperature.

The content of sulfur was evaluated using Elementar vario EL Cube (Elementar) in the CHNS module.

The scanning electron microscopy (SEM) was performed on Tescan Lyra 3 (Tescan, CZ).

Temperature programmed desorption (TPD) of pyridine was carried out using AutoChem II 2920 (Micromeritics Instrument), both thermal conductivity detector (TCD) and quadrupole mass spectrometer (MKR Cirrus 2 Analyzer) with a capillary-coupling system were used. The samples (0.06 g) were heated in ultrahigh-purity helium (30 ml·min^{-1}) at 160 °C (1 h) to activate the surface. The adsorption temperature of pyridine was 150 °C, measured pulses of pyridine vapour (pulse volume, 5 ml) were injected into helium gas and carried through the catalyst sample until saturated adsorption. Then the sample was flushed with helium for 2 hours to remove physisorbed pyridine. Afterwards the linear temperature program (5 K·min^{-1}) started and the sample was heated up to temperature of 500 °C. The desorbed amounts of pyridine were determined by calibration of the intensity of 79 amu MS response.

GC analyses of reaction mixture samples were performed on (i) Shimadzu GC 2010 chromatograph equipped with a flame ionisation detector and non-polar column ZB-5 (Zebron) (for Prins cyclization and esterification); (ii) Shimadzu GC-17A chromatograph equipped with a flame ionization detector and polar column Stabilwax-DB (Restek) (for cyclization of citronellal). Identification of product structures in reaction mixtures were performed using Shimadzu GC 2010 Plus chromatograph equipped with a mass spectrometer Shimadzu GC-MS QP 2010 Ultra and non-polar column ZB-1 (Zebron).

Acknowledgements

We acknowledge grant project GACR 17-03474S and GAUK 210119. This work was realized within the Operational Programme Prague – Competitiveness (CZ.2.16/3.1.00/24501) and "National Program of Sustainability" ((NPU I LO1613) MSMT-43760/2015), and we also acknowledge Specific University Research project (MSMT No 21-SVV/2019). This work has also been supported by Charles University Research Centre program No. UNCE/SCI/014.

Keywords: catalysis•cyclization•sulfonation•porous polymer catalysts•hyper-cross-linked

[1] H. Bohra, P. Li, C. Yang, Y. Zhao, M. Wang, *Polym. Chem.* **2018**, *9*, 1972–1982.

[2] G. Deng, Z. Wang, *Macromol. Rapid Commun.* **2018**, *39*, 1700618.

[3] Y.-B. Zhou, Z.-P. Zhan, *Chem. – An Asian J.* **2018**, *13*, 9–19.

[4] K. Dong, Q. Sun, X. J. Meng, F. S. Xiao, *Catal. Sci. Technol.* **2017**, *7*, 1028–1039.

[5] Q. Sun, Z. F. Dai, X. J. Meng, F. S. Xiao, *Chem. Soc. Rev.* **2015**, *44*, 6018–6034.

[6] S. K. Kundu, A. Bhaumik, *Acs Sustain. Chem. Eng.* **2015**, *3*, 1715–1723.

[7] P. Kaur, J. T. Hupp, S. T. Nguyen, *ACS Catal.* **2011**, *1*, 819–835.

[8] L. Sekerová, M. Lhotka, E. Vyskočilová, T. Faukner, E. Slováková, J. Brus, L. Červený, J. Sedláček, *Chem. – A Eur. J.* **2018**, *24*, 14742–14749.

[9] B. M. Antunes, A. E. Rodrigues, Z. Lin, I. Portugal, C. M. Silva, *Fuel Process. Technol.* **2015**, *138*, 86–99.

[10] S. Schlick, E. Bortel, K. Dyrek, *Acta Polym.* **1996**, *47*, 1–15.

[11] P. Drabina, J. Svoboda, M. Sedlák, *Mol.* **2017**, *22*, 865-883.

[12] J. Sedláček, M. Pacovská, D. Rédrová, H. Balcar, A. Biffis, B. Corain, J. Vohlídal, *Chem. – A Eur. J.* **2002**, *8*, 366–371.

[13] A. Corma, *Chem. Rev.* **1997**, *97*, 2373–2420.

[14] J. E. Romo, N. V Bollar, C. J. Zimmermann, S. G. Wettstein, *ChemCatChem* **2018**, *10*, 4805–4816.

[15] H. Balcar, J. Čejka, *Catal.* **2019**, *9*, 743-761.

[16] Z. Xie, C. Wang, K. E. deKrafft, W. Lin, *J. Am. Chem. Soc.* **2011**, *133*, 2056–2059.

[17] J. Chen, H. Li, M. Zhong, Q. Yang, *Green Chem.* **2016**, *18*, 6493–6500.

[18] Y. Xie, T. T. Wang, X. H. Liu, K. Zou, W. Q. Deng, *Nat. Commun.* **2013**, *4*, DOI 10.1038/ncomms2960.

[19] H. Lv, W. Wang, F. Li, *Chem. – A Eur. J.* **2018**, *24*, 16588–16594.

[20] X. Du, Y. Sun, B. Tan, Q. Teng, X. Yao, C. Su, W. Wang, *Chem. Commun.* **2010**, *46*, 970–972.

[21] V. S. Mothika, P. Sutar, P. Verma, S. Das, S. K. Pati, T. K. Maji, *Chem. – A Eur. J.* **2019**, *25*, 3867–3874.

[22] Y. Lan, C. Yang, Y. Zhang, W. An, H. Xue, S. Ding, P. Zhou, W. Wang, *Polym. Chem.* **2019**, *10*, 3298–3305.

[23] X. Wang, X. Zhao, W. Dong, X. Zhang, Y. Xiang, Q. Huang, H. Chen, *J. Mater. Chem. A* **2019**, *7*, 16277–16284.

[24] L. Havelková, A. Hašková, B. Bashta, J. Brus, M. Lhotka, E. Vrbková, M. Kindl, E. Vyskočilová, J. Sedláček, *Eur. Polym. J.* **2019**, *114*, 279–286.

[25] S. Bhunia, B. Banerjee, A. Bhaumik, *Chem. Commun.* **2015**, *51*, 5020–5023.

[26] R. M. N. Kalla, M. R. Kim, I. Kim, *Ind. Eng. Chem. Res.* **2018**, *57*, 11583–11591.

[27] R. M. N. Kalla, S. S. Reddy, I. Kim, *Catal. Letters* **2019**, *149*, 2696–2705.

[28] J. Guadalupe, A. M. Ray, E. M. Maya, B. Gómez-Lor, M. Iglesias, *Polym. Chem.* **2018**, *9*, 4585–4595.

[29] R. Gomes, P. Bhanja, A. Bhaumik, *J. Mol. Catal. A: Chem.* **2016**, *411*, 110–116.

[30] M. Du, A. M. Agrawal, S. Chakraborty, S. J. Garibay, R. Limvorapitux, B. Choi, S. T. Madrahimov, S. T. Nguyen, *ACS Sustain. Chem. Eng.* **2019**, *7*, 8126–8135.

[31] S. Chakraborty, Y. J. Colón, R. Q. Snurr, S. T. Nguyen, *Chem. Sci.* **2015**, *6*, 384–389.

[32] E. Slováková, A. Zukal, J. Brus, H. Balcar, L. Brabec, D. Bondarev, J. Sedláček, *Macromol. Chem. Phys.* **2014**, *215*, 1855–1869.

[33] E. Slováková, M. Ješelnik, E. Žagar, J. Zedník, J. Sedláček, S. Kovačič, *Macromolecules* **2014**, *47*, 4864–4869.

[34] V. Hankova, E. Slovakova, J. Zednik, J. Vohlidal, R. Sivkova, H. Balcar, A. Zukal, J. Brus, J. Sedlacek, *Macromol. Rapid Commun.* **2012**, *33*, 158–163.

[35] X. Wang, L. Zhang, Z. Guo, Y. Shi, Y. Zhou, J. Wang, *Appl. Surf. Sci.* **2019**, *478*, 221–229.

[36] T. Sakaguchi, K. Kameoka, T. Hashimoto, *J. Polym. Sci. Part A:Polym. Chem.* **2009**, *47*, 6463–6471.

[37] T. Sakaguchi, T. Hashimoto, *Polym. J.* **2014**, *46*, 391–398.
[38] E. Vyskočilová, M. Malý, A. Aho, J. Krupka, L. Červený, *React. Kinet. Mech. Catal.* **2016**, *118*, 235–246.
[39] E. Vyskočilová, J. Dušek, M. Babirádová, J. Krupka, I. Paterová, L. Červený, *Res. Chem. Intermed.* **2018**, *44*, 3971–3984.
[40] E. Selli, L. Forni, *Micropor. Mesopor. Mater.* **1999**, *31*, 129–140.
[41] Sigma Aldrich, Product specification "Amberlyst 15 hydrogen form - wet, moisture ~ 48%," can be found under [https://www.sigmaaldrich.com/Graphics/COfAInfo/SigmaSAPQM/SPEC/21/216399/216399-BULK_____ALDRICH__.pdf]; **2019**.
[42] J. Béssiere, *Anal. Chim. Acta* **1970**, *52*, 55–63.
[43] F. Liu, W. Kong, Ch. Qi, L. Zhu, F.-S. Xiao, *ACS Catal.* **2012**, 2, 565-572.
[44] J. Fu, L. Chen, P. Lv, L. Yang, Z. Yuan, Fuel **2015**, 154, 1-8.
[45] I. K. Mbaraka, D. R. Radu, V. S.-Y. Lin, B. H. Shanks, *J. Catal.* **2003**, *219*, 329–336.
[46] K. Suwannakarn, E. Lotero, J. G. Goodwin, *Ind. Eng. Chem. Res.* **2007**, *46*, 7050–7056.
[47] L. Sekerova, H. Cerna, E. Vyskocilova, L. Cerveny, *React. Kinet. Mech. Catal.* **2019**, *126*, 869–878.
[48] L. Sekerova, E. Vyskocilova, J. S. Fantova, I. Paterova, J. Krupka, L. Cerveny, *Res. Chem. Intermed.* **2017**, *43*, 4943–4958.
[49] E. Vyskocilova, L. Rezkova, E. Vrbkova, I. Paterova, L. Cerveny, *Res. Chem. Intermed.* **2016**, *42*, 725–733.
[50] E. Vyskocilova, M. Kratka, M. Vesely, E. Vrbkova, L. Cerveny, *Res. Chem. Intermed.* **2016**, *42*, 6991–7003.
[51] M. Stekrova, P. Maki-Arvela, N. Kumar, E. Behravesh, A. Aho, Q. Balme, K. P. Volcho, N. F. Salakhutdinov, D. Y. Murzin, *J. Mol. Catal. A: Chem.* **2015**, *410*, 260–270.
[52] L. Sekerova, E. Vyskocilova, L. Cerveny, *React. Kinet. Mech. Catal.* **2017**, *121*, 83–95.
[53] H. Buschmann, H. D. Scharf, *Synthesis-Stuttgart* **1988**, *1988*, 827–830.
[54] G. K. Chuah, S. H. Liu, S. Jaenicke, L. J. Harrison, *J. Catal.* **2001**, *200*, 352–359.
[55] P. R. S. Braga, A. A. Costa, E. F. de Freitas, R. O. Rocha, J. L. de Macedo, A. S. Araujo, J. A. Dias, S. C. L. Dias, *J. Mol. Catal. A: Chem.* **2012**, *358*, 99–105.

10.1002/cctc.201901815

WILEY-VCH

FULL PAPER

Highly sulfonated hyper-cross-linked polyacetylene networks with permanent porosity and specific surface area about 550 $m^2 \cdot g^{-1}$ were prepared and successfully used in esterification and Prins cyclization as reusable acid heterogeneous catalysts.

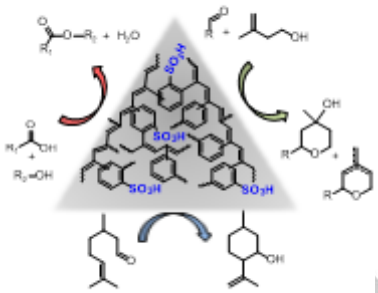

Lada Sekerová, Pavlína Březinová, Thuy Tran Do, Eliška Vyskočilová*, Jiří Krupka, Libor Červený, Lucie Havelková, Bogdana Bashta, Jan Sedláček*

Page 1-12

Sulfonated hyper-cross-linked porous polyacetylene networks as versatile heterogeneous acid catalysts